Overview of recent snowflake divertor studies in TCV

B. Labit, G.P. Canal, T. Lunt[1], H. Reimerdes, W.A.J. Vijvers, S. Coda, B.P. Duval, G. De Temmerman[2], T.W. Morgan[2], B. Tal[3] and the TCV team

Ecole Polytechnique Fédérale de Lausanne (EPFL), Centre de Recherches en Physique des Plasmas (CRPP), CH-1015 Lausanne, Switzerland [1]*Max-Planck Institut für Plasmaphysik, Garching, Germany* [2]*FOM DIFFER, Nieuwegein, The Netherlands* [3]*WIGNER RCP, RMKI, Budapest, Hungary*

This contribution describes the results of recent TCV experiments dedicated to the validation of the projected advantages of the snowflake (SF) divertor configuration. The SF configuration has been proposed as an alternative to the conventional single-null (SN) divertor to decrease the power flux to the divertor targets in a fusion reactor.

Geometrical properties of the snowflake divertor in TCV – A set of equilibria using the SPIDER equilibrium solver has been created for the three variants of a snowflake divertor with σ=0.5: SF_+ (θ=90^o), SF_-^{LFS} (θ=30^o) and SF_-^{HFS} (θ=150^o). For both targets (HFS and LFS), the flux expansion at the targets $f_{exp,t}$, the connection lengths C_l and the minimal distance of a flux surface to the primary x-point ρ_{npt} are computed as a function of the upstream coordinate at the outboard midplane $\rho_u = R - R_{LCFS}$ and compared in Fig.1 with a single-null (SN) equilibrium (σ=1.5). For these four cases, $|\nabla B_{\theta,npt}| \sim$0.2 T/m. The target flux expansion $f_{exp,t}$ for the SF cases never exceeds the value obtained for the SN divertor. This occurs because the divertor targets in TCV are located far from the null-region (Fig. 2) and so are not optimized to take advantage of the increased flux expansion that mostly occurs close to the null-point.

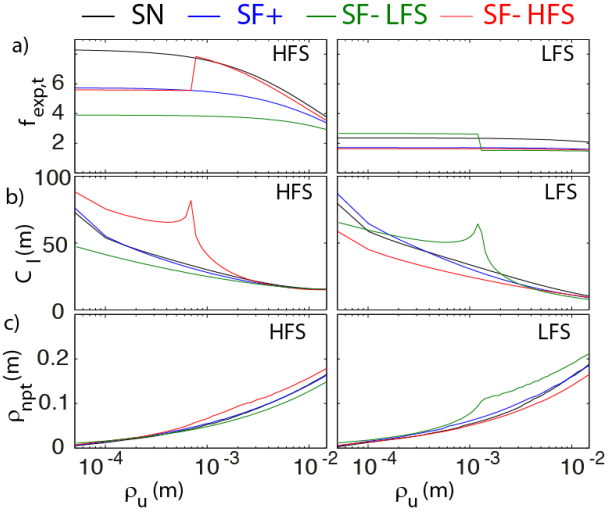

Figure 1: *Main geometrical properties of a set of equilibria as a function of ρ_u for the inner and outer targets: a) $f_{exp,t}$, b) C_l and c) ρ_{npt}.*

A significant increase of the connection length is expected for both SF_- configurations up to ρ_u=1 mm. The increase is moderate for the SF_+ and restricted to an even thinner part of the SOL. Outside this region, C_l is shorter for any SF configuration compared to the SN case. Since this region is significantly smaller than the typically observed SOL width ($\sim$8 mm) in TCV, it is not expected to gain a significant advantage from an increased C_l in the SF configuration. The main feature which is expected to be beneficial in the TCV SF configurations is an increased ρ_{npt}, which is closely related to the divertor volume. The value of ρ_{npt} exceeds its value in a SN configuration across almost the entire SOL width. However, in the SF configuration, the decrease of the angle between the primary divertor legs and the separatrix enclosing the plasma, in addition to the recompression of the field lines close to the targets, overcomes the increase of ρ_{npt} in the null-point region so that

the total SOL volume of the TCV SF configuration is slightly smaller compared with a SN.

Effect of the divertor configuration on the particle flux fluctuations – In steady-state L-mode [1] or during transient events like ELMs [2], the observed power repartition between the four strike points of SF plasmas cannot be explained with parallel transport alone. Cross-field transport of particles and heat is required. In the following, we are investigating the statistical properties of particules flux fluctuations measured in the vicinity of SP1 and SP4 under attached divertor conditions ($\langle n_e \rangle = 1.5 \times 10^{19}\ m^{-3}$). In Fig. 2, four different TCV equilibria are shown, defining the divertor configurations with primary and secondary strike points. TCV is equipped with 96 flush-mounted Langmuir probes (LP) embedded in the graphite tiles. In the present set of experiments, LPs are operated with a constant voltage to measure the ion saturation current with a sampling rate of 200 kHz. Figure 2e) shows two examples of measured signals where the intermittent nature of plasma density fluctuations is clearly visible.

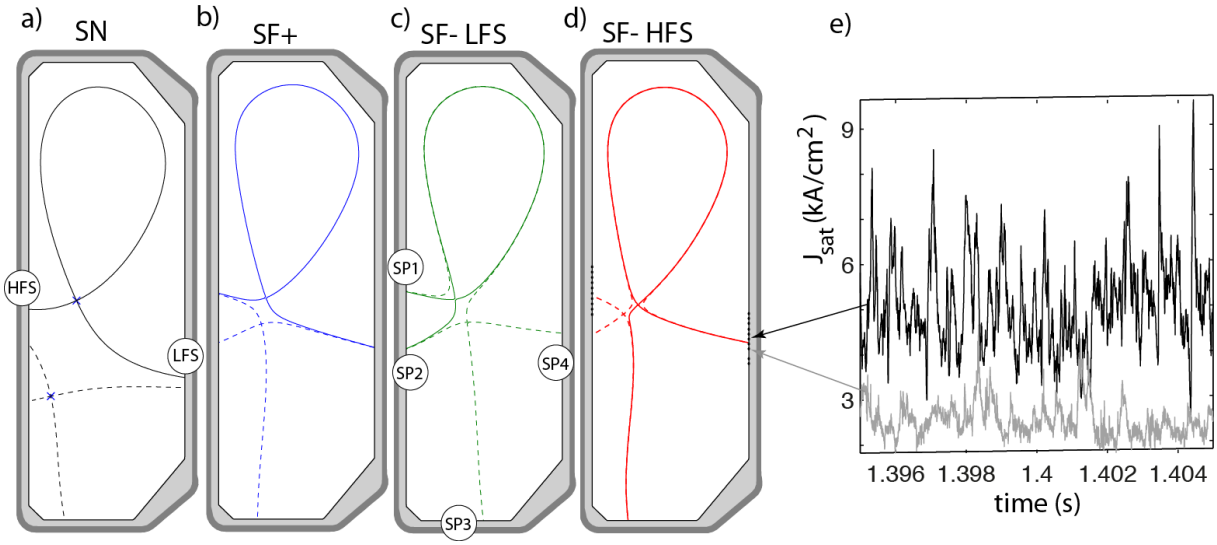

Figure 2: *Divertor configurations with primary (solid) and secondary (dashed) separatrices: a) SN SF-like ($\sigma = 1.4$), b) SF+, c) SF- LFS and d) SF- HFS, e) measured* J_{sat} *around SP4 with 2 Langmuir probes, one in the SOL, the other in the private flux region.*

Normalizing J_{sat} as $(J_{sat} - \mu_J)/\sigma_J$ where μ_J and σ_J are the time average and the standard deviation, respectively, the probability distribution function (PDF) is computed. The analysis is restricted to the probes lying either in the SOL ($0.5 \leq Z - Z_{SP} \leq 2$ cm) or in the private flux region (PFR) ($-2 \leq Z - Z_{SP} \leq -0.5$ cm). Results are shown in Fig.3. In the SOL (Fig.3a-b)), the PDF are positively skewed which is a clear signature of intermittent events and consistent with the statistical properties measured in the upstream SOL [3]. As expected from the SOL parameters study above, the PDF does not change with the divertor configuration. In the PFR, intermittency is also observed at SP1 while at SP4, bursty events are only detected for the SF_{-}^{LFS} divertor configuration. For other configurations, the plasma density fluctuations are distributed closer to the Gaussian distribution (Fig.3d)).

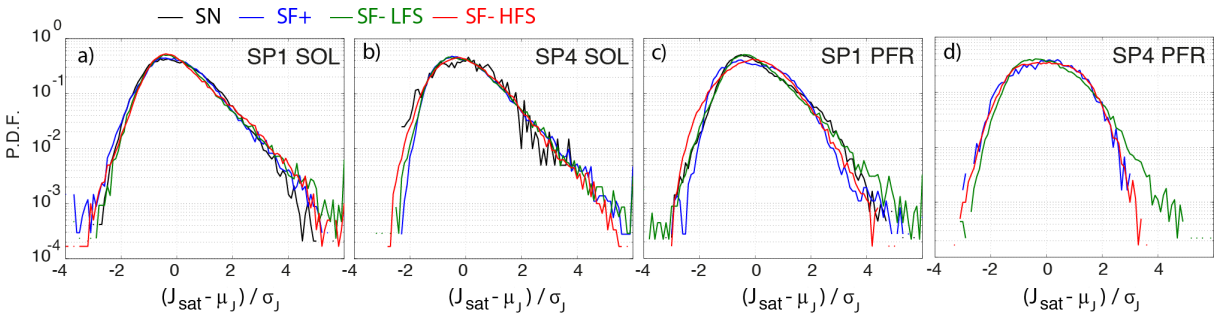

Figure 3: *Probability distribution function of normalized J_{sat} for the 4 divertor configurations at SP1 a-c) and SP4 b-d).*

Effect of plasma density on target profiles – When the plasma density is increased, the shape of the target profile at SP1 changes from a single-peaked profile to a double-peaked profile. This second peak, located in the SOL, increases with density and becomes dominant at high density [5]. The same effect is also present in the SN configuration but less pronounced. The profile shape at SP4 is almost unaffected by the plasma density increase. At SP4, the recycling current continously increases with plasma density up to the density limit while for SP1, a roll-over is observed at $\langle n_e \rangle \simeq 6 \times 10^{19}\ m^{-3}$ in the SN and at $\langle n_e \rangle \simeq 8 \times 10^{19}\ m^{-3}$ for the SF+ configuration. This can be seen as a first sign of detachment at this strike point. During a density scan, we are measuring J_{sat} fluctuations around strike points SP1 and SP4, using the Langmuir probes. This has been done for a SF+ and a SF-LFS diverted plasmas. The PDF of the normalized J_{sat} shows that, at higher density, the number of burst events reduces in the SOL. In the PFR of SP4, both PDFs for SF_+ and SF_-^{LFS} are of gaussian shape at high density while they strongly differ at low density. A clear effect of the plasma density is seen in the SP1 PFR where the number of negative density fluctuations is strongly reduced at high density. This might be related to the physical mechanism at work when a plasma starts to detach.

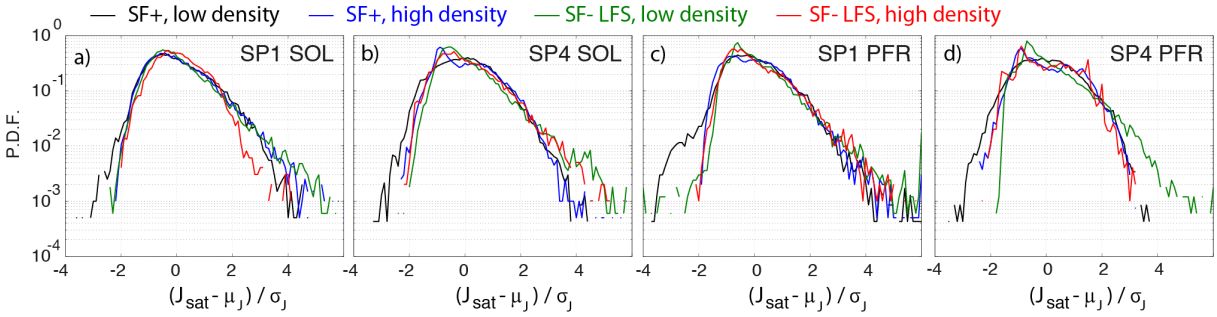

Figure 4: *PDF of normalized J_{sat} at low and high plasma densities at SP1 a-c) and SP4 b-d).*

Effects of drifts on the target profiles – Numerical simulations of TCV SF plasmas with the EMC3-Eirene code clearly demonstrated that cross-field diffusion alone is not enough to explain to experimental SOL power repartition [4]. A mechanism based on the $E \times B$ particle drift is proposed to contribute to this enhanced cross-field transport [5]. To estimate the importance of this transport channel, both poloidal and cross-field components of the electric field are computed with the steady-state kinetic profiles calculated in the simulations of n_e, T_e and T_i. A qualitative picture of the $E \times B$ drift transport is shown in Fig.5 for forward and reversed

B_ϕ. This convective transport is predicted to be enhanced at larger values of plasma density and smaller σ. These predictions are consistent with the experimentally measured heat and particle flux profiles at the targets, in particular explaining the observed asymmetry in the target profiles at SP3.

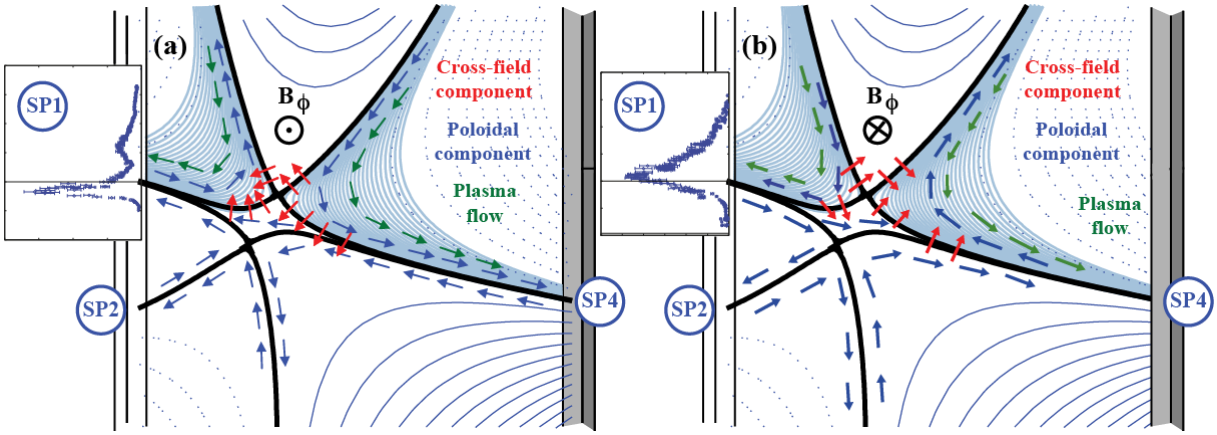

Figure 5: *Schematic of the $E \times B$ drift transport in the SF+ divertor for a) forward and b) reversed B_ϕ. The insets show the measured density profiles.*

Radiative snowflake divertor experiments – Another predicted advantage of the SF configuration is based on its larger divertor volume, which should facilitate the conversion of particle energy into radiation and thereby access to detachment. Experiments were carried out to compare the plasma response to Neon impurity seeding, in Ohmically heated SF+ and SN configurations. For the same amount of injected Neon, the plasma in the SF+ configuration radiates approximately 15% more power than in a conventional configuration. With Neon seeding, the radiated power fraction $f_{\text{rad}} = P_{\text{rad}}/P_\Omega$ could be increased up to 70%. Accordingly, the power flux due to the plasma at the strike points decreased mainly because of a broadenning of the profiles. In the SN case, the radation region is located close to the inner target, while for the SF+ divertor, the radiation zone is significantly larger, extending past the divertor null region further uptstream. In these Ohmic TCV discharges, the radiated fraction is limited by the onset of a low wavenumber MHD instability rather than a radiation instability. More details about these experiments, including a comparison with plasma density as radiator, can be found in [6].

This work was supported in part by the Fonds National de la Recherche Scientifique and in part by EURATOM within the framework of the EFDA PPPT Work Programme. The views and opinions expressed herein do not necessarily reflect those of the European Commission.

[1] H. Reimerdes *et al*, 2013 Plasma Phys. Control. Fusion **55** 124027.
[2] W.A.J. Vijvers *et al*, 2014 Nucl. Fusion **54** 023009
[3] B. Labit *et al*, Proceedings of the 38th Conference on Plasma Physics - European Physical Society, Strasbourg, France, 2011, P2.076
[4] T. Lunt *et al*, 2014 Plasma Phys. Control. Fusion **56** 035009
[5] G. P. Canal, *Sawtooth generated magnetic islands and the properties of the snowflake divertor*, EPFL PhD thesis n^{o} 6272, 2014, submitted http://dx.doi.org/10.5075/epfl-thesis-6272
[6] H. Reimerdes *et al*, *Experimental investigation of neon seeding the the snowflake configuration in TCV*, 21st PSI conference, Kanazawa, Japan, 2014, submitted to J. Nucl. Mat.